Air flow structures in the very close vicinity of wind generated water waves

Hubert Branger, Laurent Grare, William L. Peirson

▶ To cite this version:

Hubert Branger, Laurent Grare, William L. Peirson. Air flow structures in the very close vicinity of wind generated water waves. International Conference on Fluxes and Structures in Fluids, Jun 2013, San-Petersburg, Russia. 3pp. hal-00856102

HAL Id: hal-00856102
https://hal.science/hal-00856102

Submitted on 30 Aug 2013

HAL is a multi-disciplinary open access archive for the deposit and dissemination of scientific research documents, whether they are published or not. The documents may come from teaching and research institutions in France or abroad, or from public or private research centers.

L'archive ouverte pluridisciplinaire **HAL**, est destinée au dépôt et à la diffusion de documents scientifiques de niveau recherche, publiés ou non, émanant des établissements d'enseignement et de recherche français ou étrangers, des laboratoires publics ou privés.

AIR-FLOW STRUCTURE IN THE VERY CLOSE VICINITY OF WIND GENERATED WATER-WAVES

Hubert Branger[1], Laurent Grare[2] and Bill Peirson[3]

1: IRPHE, CNRS, UMR 7342, Campus Luminy, Case 903, 13009 Marseille, France, branger@irphe.univ-mrs.fr

2 : Scripps Institution of Oceanography, Marine Physical Laboratory, University of California San Diego, La Jolla, CA 92037, USA, lgrare@ucsd.edu

3 : Water Research Laboratory, School of Civil and Environmental Engineering, University of New South Wales, King St., Manly Vale NSW 2093 AUSTRALIA, W.Peirson@unsw.edu.au

In the large wind-wave tank of IRPHE (*40m* long, *3m* wide, *1m* deep water and *1.7m* high for the air, wind speed up to *14m/s*) we conducted a set of experiments to measure the structure of the air flow in the very close vicinity of the water-surface above wind-generated waves. We estimated momentum transfers from air to water and we made direct measurements of form drag and viscous drag quantities for different conditions of wind and waves.

The total drag from air to water is equal to : $\tau_{tot} = \rho_{air}\,\overline{uw} = \rho_{air}\,u*^2$, with ρ_{air} the air-density, u and w the horizontal and vertical components of the wind speed, $u*$ the friction velocity, and the bar denotes the time-average. The momentum flux does not vary with the altitude *z*, and at the water surface $z = \eta$, the total drag is equal to the sum of the viscous drag τ_υ and the form drag τ_{form}:

$$\tau_{tot} = \rho_{air}\,u*^2 = \tau_\upsilon + \tau_{form} = \rho_{air}\,\upsilon_{air}\,({}^{\partial u}/_{\partial z})_{z=\eta} + (\overline{P(\partial\eta/\partial x)})_{z=\eta}$$

with P the static pressure, $\partial\eta/\partial x$, the slope of the water waves, $\upsilon_{air}$the air kinematic viscosity.

Wave characteristics were measured with a set of conventional capacitance wave gauges, and the total momentum transfer τ_{tot} was determined with hot X-wire anemometer probes. Measured constant vertical profiles of τ_{tot} demonstrated the existence of a constant flux layer above the water surface. In order to estimate the form drag and the viscous drag at the sea surface, we build two new microphysical devices:

1) the wind-speed vertical-profile was measured down to the surface with a specialist *kingfisher* apparatus: this device carries a single 5µm diameter hot wire and undertakes a rapid vertical wind profile downwards to the water surface. While acquiring horizontal wind speed data every 50µm, the hot-wire hits the water surface. An example of the vertical profile of the normalized phase-averaged wind-speed in the air-viscous layer (1mm above water surface) is shown on Fig 1. Viscous drag for different wind speeds are shown in Fig 2.

2) static pressure fluctuations at a constant curvilinear altitude above waves, were measured with an very sensitive piezo-pressure sensor (precision $\pm 0.2\ Pa$) located inside an Eliot disk antenna. This sensor was put on a new *wave-follower* device. A capacitance wave gauge output signal was connected to the wave-follower actuator command via a signal conditioning which controlled the gain, sensitivity, speed and acceleration of the following rod, thus resulting in an accurate constant elevation of the pressure probe above the surface (more details on the devices, sensors and results can be found in [1] and [2]). Examples of wave-phase-averaged static pressure field and form drag τ_P are shown in Fig 3.

At the water surface, the wind-drift current is mainly induced by the viscous drag, and the wave height amplification is mainly induced by the form drag. The partition of the total drag into viscous drag and form drag was studied in [1]. Fig. 4 and 5 show examples of variation of the drags with wind speed and wave steepness *ak* (*a* amplitude, k wavenumber). Our work shows that wave coherent tangential stress may be more important at low *ak*.

We quantified also the associated growth rate of the surface wave fields. The systematic energy budgets for the interaction between wind and waves are detailed in [1] and will be presented during the oral session.

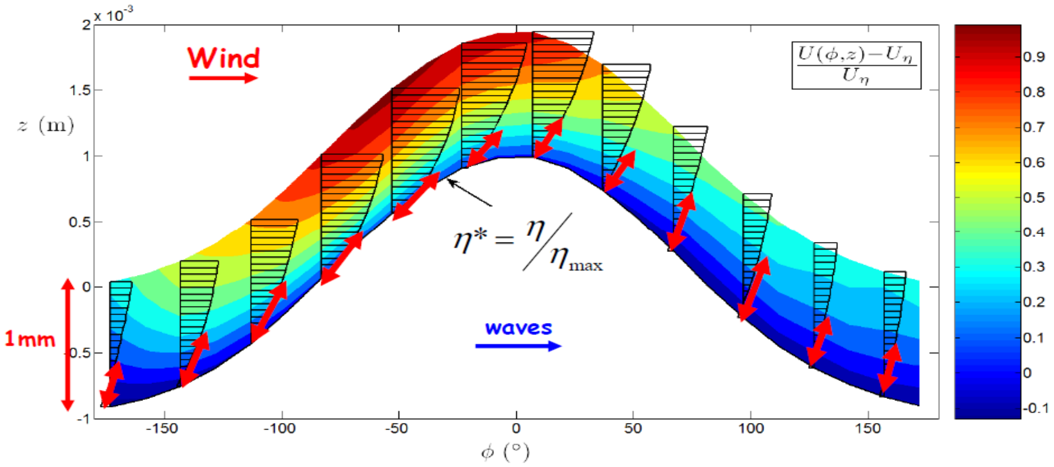

Fig 1. Results from the kingfisher device: vertical profile of the normalized phase-averaged wind-speed in the air-viscous layer (1mm above water surface). Wind speed 7m/s, mean wavelength L=0.48m

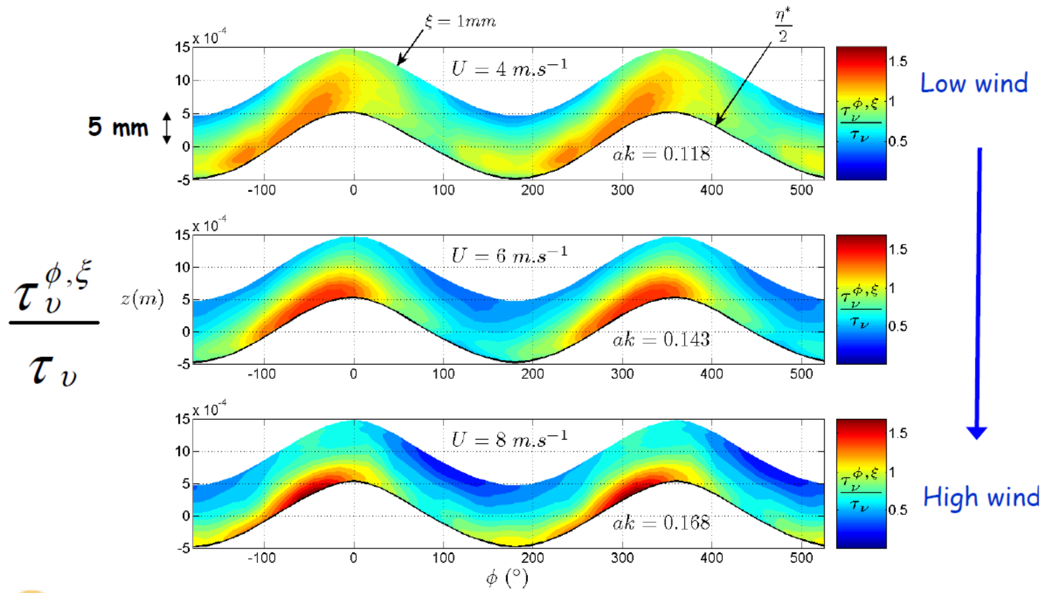

Fig 2. Normalized phase-averaged viscous drag above waves for different wind speed. Wind above the waves blows from left to the right.

REFERENCES

1. *Grare L., Peirson W., Branger H, Walker J., Giovanangeli J.P, Makin V.* Growth and dissipation of wind forced, deep water waves // J. Fluid Mech. 2013. in press.
2. *Grare L.*, Ocean-Atmosphere interaction study in the vicinity of water surface: application to wind waves and rogue waves // Ph. D. thesis, 2010, Aix-Marseille University, P 1-222, available on request by mail at lgrare@ucsd.edu
3. *Makin V., Branger H., Peirson W., Giovanangeli J-P.* Modelling of laboratory measurements of stress in the air flow over wind-generated and paddle waves // J. Phys. Oceano. 2007. V. 37. P. 2824–2837.

4. *Peirson W., Garcia A.* On the wind-induced growth of slow water waves of finite steepness. J. Fluid Mech. 2008. V. 608. P. 243–274.

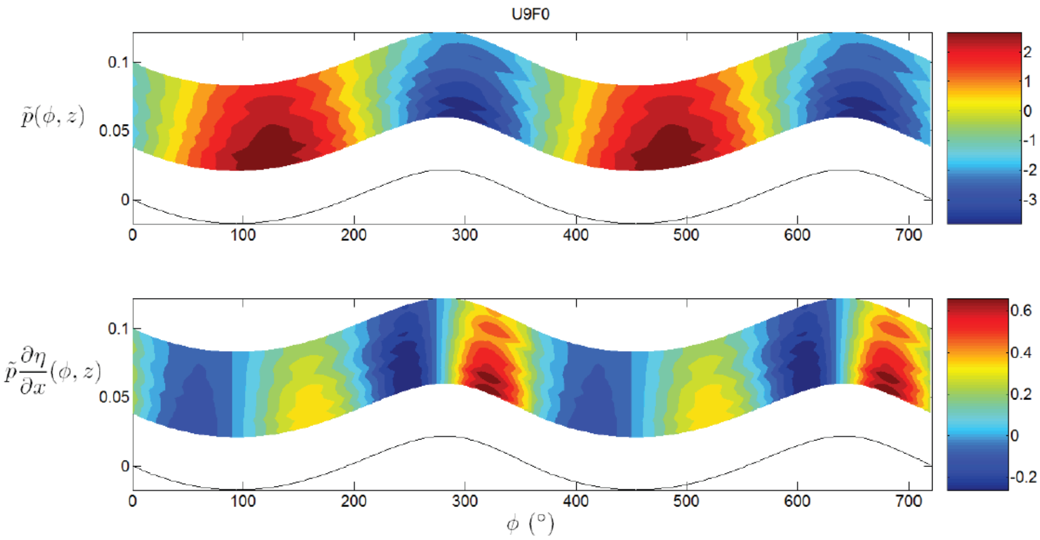

Fig 3. Examples of fluctuating phase-averaged static pressure field and form-drag measurements obtained with the Piezo sensor and Eliot antenna located on the wave follower.Units in Pa. Wind (9m/s) is blowing from left to right. Mean wavelength L=0.61m

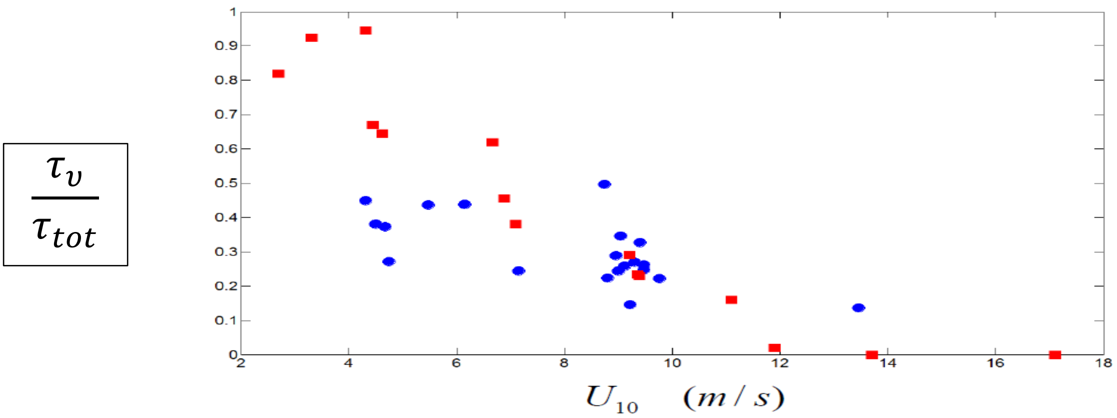

Fig 4: variation of the "viscous drag /total drag" ratio with wind speed. Blue dots: direct measurements, red squares: Makin's model [3].

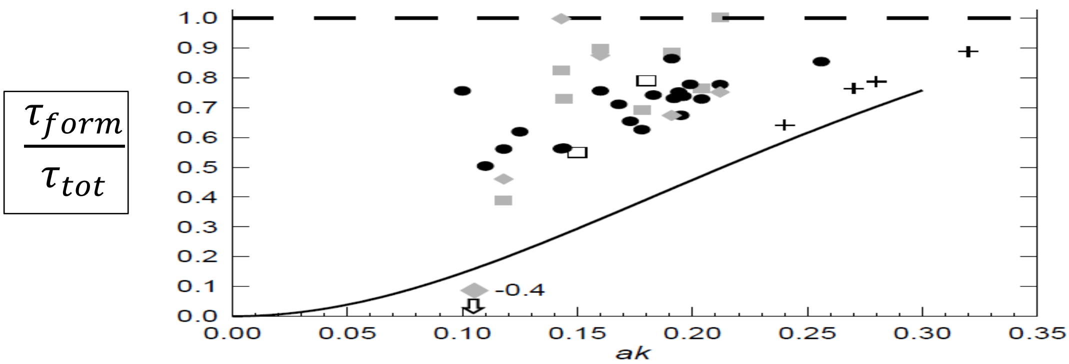

Fig 5: variation of the "form drag/total drag" ratio with wave steepness: black dots: direct measurements, other symbols: data from other studies (see [1]), black curve obtained from the net measurement of Peirson and Garcia [4].